Journal of chemical & engineering data

pubs.acs.org/jced Article

Two-Phase and Vapor-Phase Thermophysical Property (*pvTz*) Measurements of the Difluoromethane + *trans*-1,3,3,3-Tetrafluoroprop-1-ene Binary System

Sebastiano Tomassetti, Uthpala A. Perera, Giovanni Di Nicola,* Mariano Pierantozzi, Yukihiro Higashi, and Kyaw Thu

Cite This: *J. Chem. Eng. Data* 2020, 65, 1554−1564 Read Online

ACCESS | Metrics & More | Article Recommendations

ABSTRACT: In this paper, 182 *pvTz* data (28 data in the two-phase region and 154 data in the superheated vapor region) of mixtures containing difluoromethane (R32) and *trans*-1,3,3,3-tetrafluoroprop-1-ene (R1234ze(E)) are reported. The measurements were carried out along 10 isochores (0.013173, 0.039422, 0.043115, 0.046522, 0.062966, 0.068225, 0.068959, 0.110447, 0.115156, and 0.121732 $m^3 \cdot kg^{-1}$) in the temperature range from 263 to 373 K for 10 R32 mole fractions (0.1677, 0.2360, 0.2551, 0.4634, 0.5374, 0.6715, 0.7383, 0.7544, 0.9532, and 0.9533). The flash method with three equations of state (EoSs) was used to assess the vapor−liquid equilibrium of the binary mixture under analysis. The calculated vapor−liquid equilibrium behavior for the R32 + R1234ze(E) binary system agreed with the experimental data collected from the open literature. The vapor-phase measurements were correlated through the aforementioned EoSs and a truncated virial EoS. These *pvTz* points agreed with both the values provided by the EoSs and REFPROP 10.0.

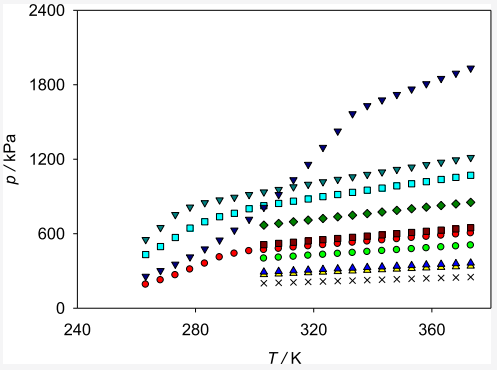

INTRODUCTION

Recently, the heating, ventilation, air conditioning, & refrigeration (HVAC&R) industry has taken steps to combat its direct contributions to climatic issues such as global warming through the reduction and phase-out of high global warming potential (GWP) refrigerants which include hydrofluorocarbons (HFCs). This has been a cumulative result of both international treaties such as the 2016 Kigali Amendment to the Montreal Protocol[1] and the ratification of the Paris Agreement[2] and several national level environmental regulations and legislations which hope to combat the emission of fluorinated greenhouse gasses (GHGs). Pertaining to the latter, the European Union (EU) and Japan have been taking many steps toward controlling the emissions of fluorinated gas (F-gas) through local level policies. The latest addition to the multitude of regulations within the EU is the F-Gas regulation (EU) no. 517/2014[3] which sets limits to the yearly allowable sales and emissions of GHGs. However, in Japan, the revised F-gas act of 2015[4] focused specifically on setting GWP targets for the industry in the hopes of promoting and moving toward market-oriented low GWP alternatives. These actions signify the commitment of the EU and Japan, like many other nations, to combat the global warming through the control of and eventual phase out of high GWP HFCs and other GHGs. The HVAC&R industry is taking steps to contribute to these efforts in order to limit the global temperature increase to below 1.5° C, by searching for the next generation of refrigerants which have zero ozone depletion potential (ODP) and very low GWP. Many institutes are thus focusing on both the development of alternative low GWP refrigerants and mixtures, and programs have been created for the continued research on their performance characteristics and properties.[5,6] McLinden et al.[7,8] and Domanski et al.[9] performed a systematic and complete analysis of an extensive database of potential low GWP refrigerants in three studies conducted in 2014 and 2017 on the basis of different criteria (environmental properties, safety, and thermodynamic performances). It was shown that only a limited group of fluids, including some hydrocarbons, inorganic compounds, and hydrofluoro olefins (HFOs), was found to present the potentially necessary characteristics for low-temperature and medium-temperature HVAC&R applications. These observations were echoed in the most recent work carried out by Bell et al.[10] in 2019, which also presented similar refrigerants for replacing R134a. From these potential low

Received: October 18, 2019
Accepted: March 3, 2020
Published: March 10, 2020

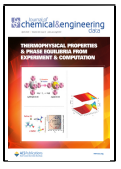

Table 1. R32 and R1234ze(E) Sample Descriptions and Molar Masses[23] (M)

chemical name	CAS number	M/g mol^{-1}	source	initial mole fraction purity	purification method	final mole fraction purity	analysis method
R32[a]	75-10-5	52.024	Ausimont SpA	0.9957	several cycles of freezing, evacuation, melting, and ultrasonic agitation	0.9998	GC
R1234ze(E)[b]	29118-24-9	114.04	Honeywell	0.995	several cycles of freezing, evacuation, melting, and ultrasonic agitation	0.999	GC

[a]Difluoromethane. [b]*trans*-1,3,3,3-Tetrafluoroprop-1-ene.

GWP alternatives, HFOs are considered as one of the most promising groups because of their low GWP and low atmospheric lifetimes as a result of their C=C double bond, but many of these refrigerants in the pure form still lack certain characteristics such as low flammability and equal or better performance in comparison to their previous counterparts.[11] Hence, mixtures of conventional refrigerants and new low GWP alternatives such as HFOs are being explored in order to forgo any undesirable characteristics and to achieve required performance targets. This creates the necessity for the continued exploration of the properties and performance of such mixtures.

Among the selected low GWP refrigerants, *trans*-1,3,3,3-tetrafluoropropene (R1234ze(E)) is considered as a potential alternative to replace R410A in air-conditioning systems and as a general climate friendly next-generation refrigerant.[12,13] However, certain fallbacks were reported by Koyama et al.[12] when using R1234ze(E) as a pure drop in place of R410A in heat pump operations mainly because of the low evaporation pressure and low vapor density which cause lower coefficients of performance and volumetric capacities and by Bell et al.,[10] where the issues related to the refrigerant's flammability class A2L were pointed out because it could affect the potential substitution of R134a in chillers. To overcome the potential limitations of R1234ze(E) in its pure form and to improve its thermodynamic performance, mixtures including R1234ze(E) and HFCs are being investigated. In particular, because of its high performance, relatively low GWP, and excellent thermodynamic properties among all HFCs, R32 is considered as one of the most suitable components for low GWP refrigerant mixtures.

Studies focusing on such refrigerant mixtures involve the investigation of thermophysical properties, which is crucial for refrigeration system design and the investigation of the performance in HVAC&R applications. As shown by Bobbo et al.,[14] many studies reporting experimentally determined data for thermodynamic and transport properties of pure R1234ze(E) have been reported in the literature. R32 is also a well-explored refrigerant.[15] As for the binary mixture of R32 + R1234ze(E), there have been several research studies presented as well.[14] Jia et al.[16] measured the compressed liquid density for five compositions of this binary mixture in the temperature range from 283 to 363 K and at pressures of up to 100 MPa using a vibrating-tube densimeter. Tanaka et al.[17] measured the density and isobaric specific heat capacity of the R32 + R1234ze(E) binary system in the temperature range from 310 to 350 K and pressure range from 1.4 to 5.0 MPa with a metal-bellows calorimeter. The $pvTz$ measurements for the R1234ze(E) + R32 binary mixture at only two different mass fractions were carried out by Kobayashi et al.[18] The vapor−liquid equilibrium (VLE) measurements of the studied binary mixture were performed by Hu et al.,[19,20] Koyama et al.,[21] and Kou et al.[22] in the temperature ranges of 283.15−323.15, 243−313, and 283.15−323.14 K, respectively.

In this work, an isochoric apparatus was used to measure two-phase and vapor-phase $pvTz$ properties the of R32 + R1234ze(E) binary system. In particular, 28 data points for four R32 mole fractions and 154 data points for 10 mol fractions were measured in two-phase and superheated vapor regions, respectively. The experimental data were correlated with several equations of state (EoSs). Moreover, they were compared with the REFPROP 10.0 predictions.

EXPERIMENTAL SECTION

Details on the studied samples, the experimental setup, and the measurement procedure are provided in this section.

Materials. Table 1 gives information on the samples of difluoromethane (R32, CH_2F_2, CAS number 75-10-5) and *trans*-1,3,3,3-tetrafluoroprop-1-ene (R1234ze(E), $CF_3CH{=}CHF$, CAS number 29118-24-9). The purity of the sample was checked by gas chromatography (GC) with a thermal conductivity detector. To remove noncondensable gases, several cycles of freezing, evacuation, thawing, and ultrasonic stirring were performed on the measured samples.

Experimental Apparatus and Procedure. The experimental setup consists of an isochoric sphere and two separate thermostatic baths that operate in the low-temperature range from 210 to 298 K and the high temperature range from 303 to 390 K, respectively. Figure 1 shows a schematic view of the apparatus. The detailed descriptions of the setup and the uncertainties are reported elsewhere,[24−27] while a summary is given below.

A gravimetric method was used to prepare the refrigerant mixtures at different test compositions. For each pure

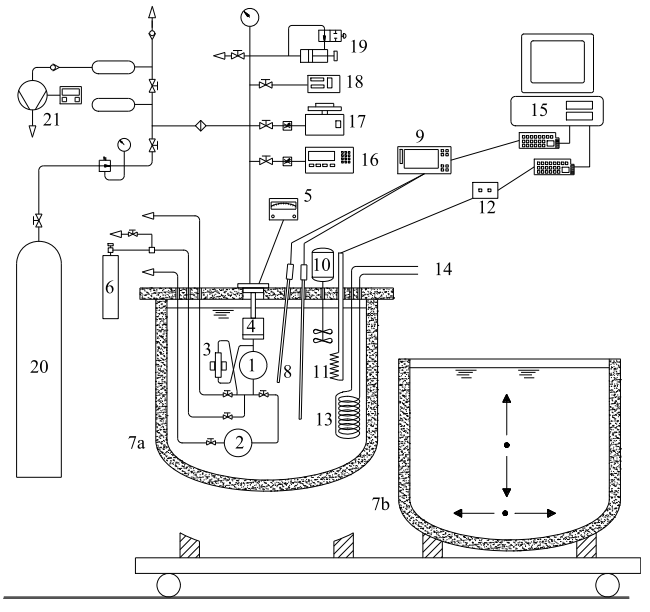

Figure 1. Schematic view of the experimental setup.

https://dx.doi.org/10.1021/acs.jced.9b00995
J. Chem. Eng. Data 2020, 65, 1554−1564

Table 2. Bulk Mole Fractions z, Average Specific Volumes v, Ranges of Temperature ΔT and Pressure Δp, Numbers of Charged Moles n, and Amounts of Charged Masses m for the R32 (1) + R1234ze(E) (2) Binary System

series	z_1	v/m^3·kg^{-1}	ΔT/K	Δp/kPa	n/mol	m_1/g	m_2/g
1	0.1677	0.046522	263.15−373.15	190.9−604.5	0.0568	0.496	5.392
2	0.2360	0.121732	303.15−373.15	200.6−250.6	0.0227	0.278	1.974
3	0.2551	0.013173	263.15−373.15	256.7−1933.5	0.2117	2.810	17.982
4	0.4634	0.068959	303.15−373.15	400.5−506.1	0.0466	1.124	2.852
5	0.5374	0.110447	303.15−373.15	271.4−339.4	0.0308	0.860	1.622
6	0.6715	0.115156	303.15−373.15	291.4−364.3	0.0329	1.149	1.232
7	0.7383	0.039422	263.15−373.15	432.1−1070.6	0.1018	3.910	3.038
8	0.7544	0.068225	303.15−373.15	512.1−648.1	0.0597	2.345	1.673
9	0.9532	0.043115	263.15−373.15	552.2−1213.9	0.1157	5.735	0.618
10	0.9533	0.062966	303.15−373.15	669.1−852.3	0.0793	3.932	0.422

Table 3. Experimental Values of Pressure p, Specific Volume v, Temperature T, and Bulk Mole Fraction z in the Two-Phase Region for the R32 (1) + R1234ze(E) (2) Binary System[a]

T/K	p/kPa	v/m^3·kg^{-1}	T/K	p/kPa	v/m^3·kg^{-1}
z_1 = 0.1677(24)			z_1 = 0.7383(5)		
263.15	190.9	0.046409(54)	263.15	432.1	0.039327(45)
268.15	226.2	0.046420(54)	268.15	496.0	0.039336(45)
273.15	266.8	0.046430(54)	273.15	569.4	0.039344(45)
278.15	312.6	0.046440(54)	278.15	645.1	0.039353(45)
283.15[b]	360.0[b]	0.046450(54)[b]	283.15[b]	696.3[b]	0.039362(45)[b]
288.15[b]	410.8[b]	0.046460(54)[b]			
z_1 = 0.2551(4)			z_1 = 0.9532(20)		
263.15	256.7	0.013142(15)	263.15	552.2	0.043011(50)
268.15	302.5	0.013144(15)	268.15	649.5	0.043020(50)
273.15	354.1	0.013147(15)	273.15	753.6	0.043030(50)
278.15	412.0	0.013150(15)			
283.15	476.6	0.013153(15)			
288.15	548.2	0.013156(15)			
293.15	628.0	0.013159(15)			
298.15	715.9	0.013162(15)			
303.15	811.8	0.013165(15)			
308.15	914.8	0.013168(15)			
313.15	1033.8	0.013170(15)			
318.15	1157.7	0.013173(15)			
323.15	1294.9	0.013176(15)			
328.15[b]	1426.2[b]	0.013179(15)[b]			

[a]Expanded uncertainties are $U(T)$ = 0.03 K and $U(p)$ = 1 kPa at the 95% confidence level. $U(v)$ and $U(z_1)$ at the 95% confidence level are reported between parentheses (the values of these expanded uncertainties are referred to the corresponding last digits of the experimental values). [b]Not considered in the parameter regression.

refrigerant, two bottles were first vacuumed in order to be used as the refrigerant bottle and recovery bottle. The required amount of refrigerant was charged into the refrigerant bottle and weighed using an analytical balance (Gibertini E42S-B) with an uncertainty of ±0.3 mg, while the vacuumed recovery bottle was also weighed. The isochoric cell and tubing were then evacuated, and both bottles were connected to the inlet of the isochoric cell. The required mass of the refrigerant was charged into the isochoric cell. However, once the refrigerant was charged and the isochoric cell was isolated, a certain amount of refrigerant would still remain in the connection tubing between the refrigerant bottle and the isolation valve of the isochoric cell. This remaining refrigerant was then recovered into the recovery bottle. The weight of these two bottles was measured again and recorded. In order to determine the charged refrigerant sample mass, the differences between the weights of the two bottles before and after the charging process were used for the calculation of both the refrigerant amount removed from the refrigerant bottle and the refrigerant remaining in the connection tubes which was collected in the recovery bottle. The difference in these values provides the refrigerant charged into the isochoric cell. The uncertainty of the charged masses for the refrigerant mixtures was calculated using the following equation based on the propagation of uncertainty

$$u(m) = \sqrt{4 \cdot u(m_b)^2} \quad (1)$$

where $u(m)$ is the uncertainty of the charged mass and $u(m_b)$ is the uncertainty of the analytical balance. The expanded uncertainty in mass with a coverage factor of 2 (95% confidence level) was found to be 1.2 mg.

The temperatures of the thermostatic baths were measured using a Hart Scientific 5680, 25 Ω platinum resistance thermometer. A Ruska 7000 pressure transducer was used to measure the pressure within the isochoric cell. The isochoric volume at 298 K was determined to be 273.3 cm^3. The method

https://dx.doi.org/10.1021/acs.jced.9b00995
J. Chem. Eng. Data 2020, 65, 1554−1564

Table 4. Experimental Temperature T, Pressure p, Specific Volume v, and Bulk Mole Fraction z in the Superheated Vapor Region for the R32 (1) + R1234ze(E) (2) Binary System[a]

T/K	p/kPa	v/m^3·kg^{-1}	T/K	p/kPa	v/m^3·kg^{-1}
z_1 = 0.1677(24)			z_1 = 0.6715(14)		
293.15[b]	440.3[b]	0.046471(54)[b]	303.15	291.4	0.114980(171)
298.15	460.0	0.046481(54)	308.15	296.6	0.115005(171)
303.15	470.1	0.046491(54)	313.15	301.9	0.115030(171)
308.15	480.1	0.046501(54)	318.15	307.1	0.115055(171)
313.15	490.0	0.046511(54)	323.15	312.4	0.115080(171)
318.15	499.9	0.046522(54)	328.15	317.6	0.115106(171)
323.15	509.6	0.046532(54)	333.15	322.8	0.115131(171)
328.15	519.3	0.046542(54)	338.15	328.0	0.115156(171)
333.15	528.9	0.046552(54)	343.15	333.2	0.115181(171)
338.15	538.5	0.046562(54)	348.15	338.5	0.115207(171)
343.15	547.9	0.046573(54)	353.15	343.7	0.115232(171)
348.15	557.4	0.046583(54)	358.15	348.9	0.115257(171)
353.15	567.0	0.046593(54)	363.15	354.0	0.115282(171)
358.15	576.4	0.046603(54)	368.15	359.2	0.115307(171)
363.15	585.7	0.046613(54)	373.15	364.3	0.115333(171)
368.15	595.1	0.046624(54)			
373.15	604.5	0.046634(54)			
z_1 = 0.2360(44)			z_1 = 0.7383(5)		
303.15	200.6	0.121545(186)	288.15[b]	736.4[b]	0.039370(45)[b]
308.15	204.2	0.121572(186)	293.15[b]	764.5[b]	0.039379(45)[b]
313.15	207.8	0.121599(186)	298.15[b]	801.0[b]	0.039387(45)[b]
318.15	211.4	0.121625(186)	303.15	825.3	0.039396(45)
323.15	215.1	0.121652(186)	308.15	843.8	0.039405(45)
328.15	218.6	0.121679(186)	313.15	861.9	0.039413(45)
333.15	222.2	0.121705(186)	318.15	879.8	0.039422(45)
338.15	225.8	0.121732(186)	323.15	898.6	0.039431(45)
343.15	229.3	0.121759(186)	328.15	915.3	0.039439(45)
348.15	232.9	0.121785(186)	333.15	932.9	0.039448(45)
353.15	236.5	0.121812(186)	338.15	950.4	0.039457(45)
358.15	240.0	0.121839(186)	343.15	967.8	0.039465(45)
363.15	243.6	0.121865(186)	348.15	985.1	0.039474(45)
368.15	247.1	0.121892(186)	353.15	1002.3	0.039483(45)
373.15	250.6	0.121919(186)	358.15	1019.4	0.039491(45)
			363.15	1036.6	0.039500(45)
			368.15	1053.5	0.039508(45)
			373.15	1070.6	0.039517(45)
z_1 = 0.2551(4)			z_1 = 0.7544(9)		
333.15[b]	1565.5[b]	0.013182(15)[b]	303.15	512.1	0.068120(85)
338.15	1630.9	0.013185(15)	308.15	521.8	0.068135(85)
343.15	1677.0	0.013188(15)	313.15	531.7	0.068150(85)
348.15	1721.2	0.013191(15)	318.15	541.6	0.068165(85)
353.15	1764.7	0.013194(15)	323.15	551.4	0.068180(85)
358.15	1807.8	0.013196(15)	328.15	561.2	0.068195(85)
363.15	1850.1	0.013199(15)	333.15	571.0	0.068210(85)
368.15	1892.0	0.013202(15)	338.15	580.7	0.068225(85)
373.15	1933.5	0.013205(15)	343.15	590.4	0.068240(85)
			348.15	600.1	0.068255(85)
			353.15	609.7	0.068270(85)
			358.15	619.4	0.068285(85)
			363.15	629.1	0.068299(85)
			368.15	638.6	0.068314(85)
			373.15	648.1	0.068329(85)
z_1 = 0.4634(11)			z_1 = 0.9532(20)		
303.15	400.5	0.068854(86)	278.15[b]	813.8[b]	0.043039(50)[b]
308.15	408.2	0.068869(86)	283.15[b]	849.0[b]	0.043049(50)[b]
313.15	415.9	0.068884(86)	288.15[b]	871.8[b]	0.043058(50)[b]
318.15	423.6	0.068899(86)	293.15[b]	893.3[b]	0.043068(50)[b]
323.15	431.2	0.068914(86)	298.15	914.7	0.043077(50)
328.15	438.8	0.068929(86)	303.15	935.6	0.043087(50)

https://dx.doi.org/10.1021/acs.jced.9b00995
J. Chem. Eng. Data 2020, 65, 1554−1564

Table 4. continued

T/K	p/kPa	v/m^3·kg^{-1}	T/K	p/kPa	v/m^3·kg^{-1}
333.15	446.4	0.068944(86)	308.15	956.3	0.043096(50)
338.15	453.9	0.068959(86)	313.15	976.9	0.043105(50)
343.15	461.4	0.068974(86)	318.15	997.3	0.043115(50)
348.15	468.9	0.068989(86)	323.15	1017.6	0.043124(50)
353.15	476.3	0.069005(86)	328.15	1037.7	0.043134(50)
358.15	483.8	0.069020(86)	333.15	1057.7	0.043143(50)
363.15	491.2	0.069035(86)	338.15	1077.6	0.043153(50)
368.15	498.8	0.069050(86)	343.15	1097.3	0.043162(50)
373.15	506.1	0.069065(86)	348.15	1117.1	0.043172(50)
			353.15	1136.6	0.043181(50)
			358.15	1156.1	0.043191(50)
			363.15	1175.5	0.043200(50)
			368.15	1194.7	0.043209(50)
			373.15	1213.9	0.043219(50)
z_1 = 0.5374(16)			z_1 = 0.9533(29)		
303.15	271.4	0.110278(161)	303.15	669.1	0.062869(77)
308.15	276.3	0.110302(161)	308.15	682.5	0.062883(77)
313.15	281.3	0.110326(161)	313.15	695.9	0.062897(77)
318.15	286.2	0.110350(161)	318.15	709.2	0.062911(77)
323.15	291.1	0.110375(161)	323.15	722.5	0.062924(77)
328.15	295.9	0.110399(161)	328.15	735.7	0.062938(77)
333.15	300.8	0.110423(161)	333.15	748.8	0.062952(77)
338.15	305.6	0.110447(161)	338.15	761.9	0.062966(77)
343.15	310.4	0.110471(161)	343.15	774.9	0.062980(77)
348.15	315.3	0.110495(161)	348.15	787.9	0.062993(77)
353.15	320.2	0.110520(161)	353.15	800.9	0.063007(77)
358.15	325.0	0.110544(161)	358.15	813.8	0.063021(77)
363.15	329.8	0.110568(161)	363.15	826.6	0.063035(77)
368.15	334.5	0.110592(161)	368.15	839.4	0.063049(77)
373.15	339.4	0.110616(161)	373.15	852.3	0.063062(77)

[a]Expanded uncertainties are $U(T)$ = 0.03 K and $U(p)$ = 1 kPa at the 95% confidence level. $U(v)$ and $U(z_1)$ at the 95% confidence level are reported between parentheses (the values of these expanded uncertainties are referred to the corresponding last digits of the experimental values). [b]Not considered in the parameter regression.

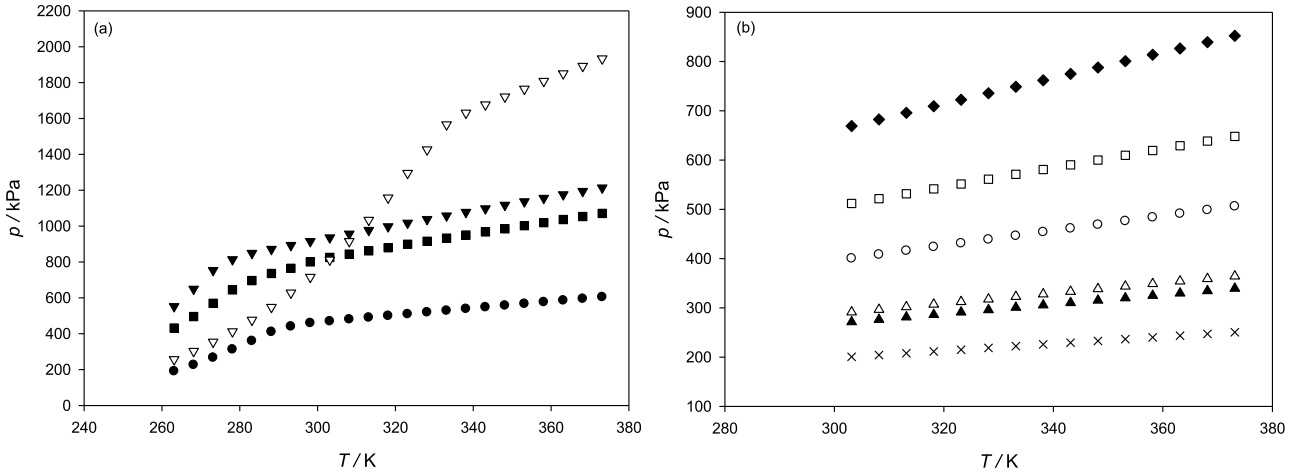

Figure 2. Pressure p, specific volume v, temperature T, and bulk mole fraction z data (Tables 3 and 4) for four R32 (1) + R1234ze(E) (2) isochores both in the two-phase and superheated vapor regions (a) and six series in the superheated vapor region (b). ●, z_1 = 0.1677 and v = 0.046522 m^3·kg^{-1}; ×, z_1 = 0.2360 and v = 0.121732 m^3·kg^{-1}; ▽, z_1 = 0.2551 and v = 0.013173 m^3·kg^{-1}; O, z_1 = 0.4634 and v = 0.068959 m^3·kg^{-1}; ▲, z_1 = 0.5374 and v = 0.110447 m^3·kg^{-1}; △, z_1 = 0.6715 and v = 0.115156 m^3·kg^{-1}; ■, z_1 = 0.7383 and v = 0.039422 m^3·kg^{-1}; □, z_1 = 0.7544 and v = 0.068225 m^3·kg^{-1}; ▼, z_1 = 0.9532 and v = 0.043115 m^3·kg^{-1}; and ◆, z_1 = 0.9533 and v = 0.062966 m^3·kg^{-1}.

used to determine the isochoric volume was based on the classic Burnett calibration procedure.[25]

As detailed elsewhere,[24] the expanded uncertainty in the temperature measurements with a coverage factor of 2 (95% coverage) was estimated to be 0.03 K. This uncertainty is due to the thermometer and the bath instability. The total uncertainty in the pressure measurements is given by four causes as follows: the contribution of the changes in

https://dx.doi.org/10.1021/acs.jced.9b00995
J. Chem. Eng. Data 2020, 65, 1554−1564

Table 5. Coefficients of the CSD EoS[28] a_i and b_i for R32 and R1234ze (E) Used in Eqs 4 and 5

fluid	a_0	a_1	a_2	b_0	b_1	b_2
R32	1662.2699	-2.1998×10^{-3}	-1.8890×10^{-6}	0.0780	-7.5238×10^{-4}	-5.3011×10^{-8}
R1234ze(E)	4161.1581	-2.5180×10^{-3}	-1.9277×10^{-6}	0.1630	-1.5315×10^{-4}	-1.4971×10^{-7}

Table 6. Two-Phase Pressures p_{calc}, Mole Fractions of the Liquid Phase $x_{1,calc}$, and Mole Fractions of the Vapor Phase $y_{1,calc}$ Estimated Through the "Flash Method" with the Selected EoSs for the Experimental Temperatures T and Bulk Mole Fraction z of the R32 (1) + R1234ze(E) (2) Binary Mixture

	CSD EoS [eq 2]			PR EoS			Stryjek EoS [eq 6]		
T/K	p_{calc}/kPa	$x_{1,calc}$	$y_{1,calc}$	p_{calc}/kPa	$x_{1,calc}$	$y_{1,calc}$	p_{calc}/kPa	$x_{1,calc}$	$y_{1,calc}$
				z_1 = 0.1677					
263.15	190.6	0.0811	0.2783	190.6	0.0811	0.2790	191.0	0.0820	0.2783
268.15	225.8	0.0757	0.2540	225.8	0.0755	0.2549	226.1	0.0764	0.2546
273.15	266.1	0.0707	0.2314	266.0	0.0703	0.2324	266.3	0.0712	0.2323
278.15	312.0	0.0660	0.2106	311.8	0.0655	0.2115	312.1	0.0663	0.2116
				z_1 = 0.2551					
263.15	255.6	0.2073	0.5225	255.1	0.2074	0.5226	254.9	0.2087	0.5213
268.15	301.1	0.2019	0.5022	300.9	0.2019	0.5029	300.7	0.2033	0.5020
273.15	352.5	0.1963	0.4817	352.4	0.1961	0.4830	352.1	0.1976	0.4824
278.15	410.0	0.1906	0.4612	410.1	0.1902	0.4628	409.8	0.1919	0.4626
283.15	474.2	0.1849	0.4406	474.5	0.1843	0.4425	474.2	0.1860	0.4427
288.15	545.5	0.1792	0.4202	546.1	0.1783	0.4221	545.7	0.1801	0.4227
293.15	624.5	0.1734	0.4001	625.2	0.1724	0.4019	624.8	0.1743	0.4027
298.15	711.7	0.1678	0.3802	712.6	0.1665	0.3818	712.2	0.1685	0.3829
303.15	807.6	0.1622	0.3606	808.8	0.1608	0.3619	808.3	0.1627	0.3633
308.15	912.9	0.1567	0.3416	914.4	0.1552	0.3424	913.8	0.1572	0.3440
313.15	1028.1	0.1514	0.3231	1030.0	0.1497	0.3234	1029.3	0.1517	0.3251
318.15	1153.8	0.1463	0.3051	1156.3	0.1445	0.3048	1155.6	0.1465	0.3067
323.15	1290.7	0.1414	0.2878	1294.0	0.1395	0.2868	1293.2	0.1415	0.2888
				z_1 = 0.7383					
263.15	435.9	0.6013	0.8396	432.7	0.6038	0.8395	432.2	0.6054	0.8400
268.15	503.7	0.5767	0.8216	500.8	0.5790	0.8216	500.3	0.5810	0.8223
273.15	576.3	0.5499	0.8008	573.9	0.5518	0.8008	573.3	0.5543	0.8018
278.15	653.4	0.5216	0.7772	651.5	0.5228	0.7771	650.9	0.5258	0.7783
				z_1 = 0.9532					
263.15	556.4	0.9243	0.9684	554.2	0.9230	0.9691	554.5	0.9228	0.9694
268.15	655.9	0.9159	0.9643	653.7	0.9141	0.9648	653.6	0.9140	0.9651
273.15	766.3	0.9041	0.9588	763.9	0.9018	0.9588	763.4	0.9018	0.9592

temperature of the thermostatic bath and the uncertainties of the transducer, the null indicator system, and the pressure gauges. Its expanded uncertainty with a coverage factor of 2 (95% coverage) was found to be 1 kPa. On the basis of the aforementioned calibration procedure, the expanded uncertainty with a coverage factor of 2 (95% coverage) for the isochoric volume was estimated to be 0.3 cm^3.

As described in the previous studies,[26,27] the uncertainty of the specific volume is a function of the uncertainties of the volume estimation and mass measurements. The expanded uncertainties in the specific volume measurement with a coverage factor of 2 (95% confidence level) for the R32 + R1234ze(E) binary system are reported in Tables 3 and 4.

On the basis of the propagation of uncertainty, the uncertainty of the mole fraction depends on the mass of the charged sample, the calculated specific volume, and the mole fraction itself.[26,27] The expanded uncertainties with a coverage factor of 2 (95% confidence level) for R32 mole fractions (z_1) of the R32 (1) + R1234ze(E) (2) binary system are reported in Tables 3 and 4.

To perform the measurements, the thermostatic bath was allowed to reach the stable conditions. At this point, a circulating pump within the isochoric cell was activated for 15 min in order to mix the sample. After waiting for about an hour for the sample to reach the equilibrium, the pressure and temperature were measured. The process was repeated for the next temperature.

RESULTS AND DISCUSSION

This section presents the $pvTz$ measurements for the R32 + R1234ze(E) binary mixture. Moreover, the results obtained by comparing the measured data with the values given by different models and the experimental data collected from the open literature are reported.

Experimental Data. The $pvTz$ measurements for mixtures containing R32 and R1234ze(E) were carried out along 10 isochores (0.013173, 0.039422, 0.043115, 0.046522, 0.062966, 0.068225, 0.068959, 0.110447, 0.115156, and 0.121732 $m^3 \cdot kg^{-1}$), for temperatures 263 < T < 373 K, and for 10 R32 mole fractions (0.1677, 0.2360, 0.2551, 0.4634, 0.5374, 0.6715, 0.7383, 0.7544, 0.9532, and 0.9533). Table 2 presents the temperature ranges, the pressure ranges, the specific volumes and the bulk mole fractions of the mixtures, the masses, and the number of moles charged for the 10 studied isochores of

https://dx.doi.org/10.1021/acs.jced.9b00995
J. Chem. Eng. Data 2020, 65, 1554−1564

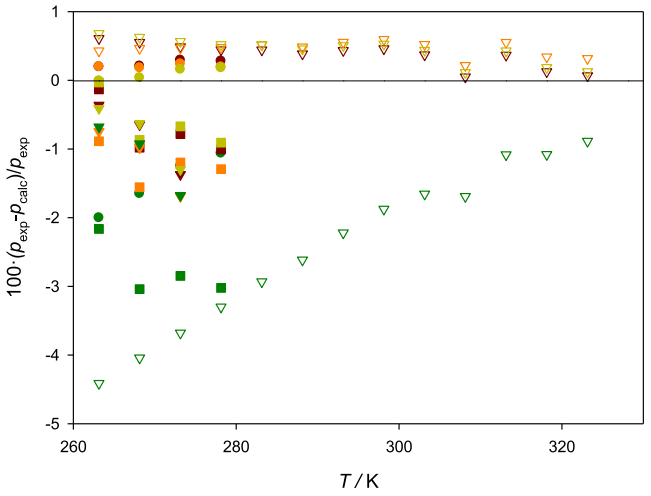

Figure 3. Deviations between experimental pressures for the R32 (1) + R1234ze(E) (2) binary system of Table 3 (p_{exp}) and values calculated (p_{calc}) from the "flash method" with the CSD EoS (a) (orange), the PR EoS (b) (wine), and a cubic EoS proposed by Stryjek (c) (green) and from REFPROP 10.0 (d) (dark green). ●, z_1 = 0.1677 and v = 0.046522 $m^3 \cdot kg^{-1}$; ▽, z_1 = 0.2551 and v = 0.013173 $m^3 \cdot kg^{-1}$; ■, z_1 = 0.7383 and v = 0.039422 $m^3 \cdot kg^{-1}$; ▼, z_1 = 0.9532 and v = 0.043115 $m^3 \cdot kg^{-1}$.

the mixtures. The two-phase and vapor-phase T, p behaviors for the 10 series are shown in Figure 2. It is possible to note from Figure 2 that six series with R32 mole fractions (0.2360, 0.4634, 0.5374, 0.6715, 0.7544, and 0.9533) were measured only in the superheated vapor region for temperatures 303 < T < 373 K. After analyzing the slope of the T, p sequences of the additional four series, the measurements were allocated either to the two-phase or superheated vapor regions. The two-phase and vapor-phase experimental data are given in Tables 3 and 4, respectively.

VLE Derivation. The VLE of the R32 + R1234ze(E) binary mixture was assessed from the two-phase isochoric measurements using the "flash method" with three different EoSs. The Carnahan−Starling−De Santis (CSD) EoS[28] was utilized in this method for VLE assessment as presented in a previous work.[29] The following form of the CSD EoS was used

$$\frac{pv_m}{RT} = \frac{1 + Y + Y^2 - Y^3}{(1 - Y)^3} - \frac{a}{RT(v_m + b)} \quad (2)$$

where

$$Y = \frac{b}{4v_m} \quad (3)$$

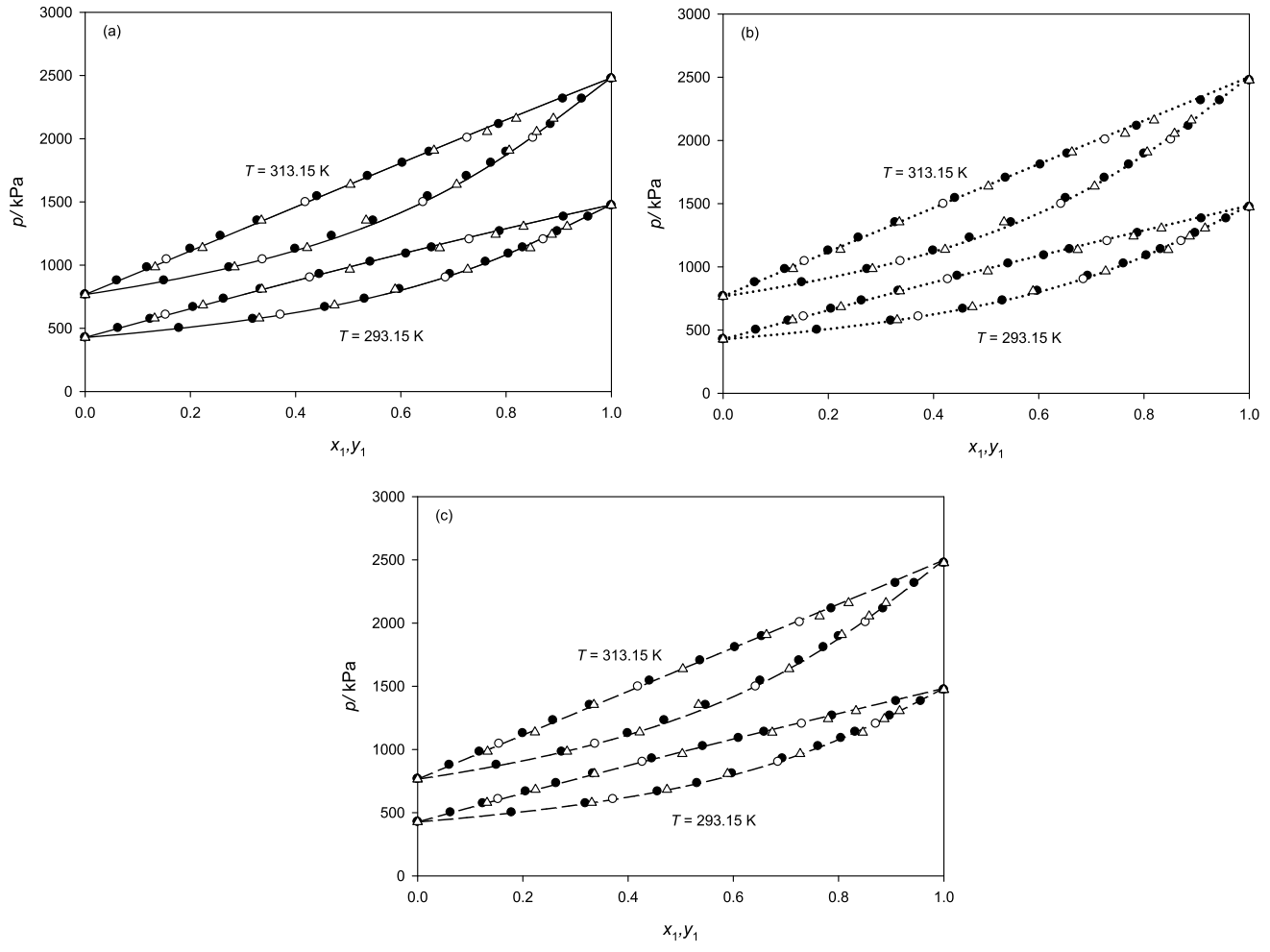

Figure 4. VLE behaviors for the R32 (1) + R1234ze(E) (2) binary mixture derived from the CSD EoS (solid lines) (a), PR EoS (dotted lines) (b), and the cubic EoS proposed by Stryjek (dashed lines) (c) at T = 293.15 K and T = 313.15 K. Black circles (●), white circles (○), and white triangles (△) are the experimental VLE values presented in Hu et al.,[19] Hu et al.,[20] and Kou et al.,[22] respectively.

https://dx.doi.org/10.1021/acs.jced.9b00995
J. Chem. Eng. Data 2020, 65, 1554−1564

Table 7. AARD (p) and AAD (y_1) Between the Experimental VLE Data Available in the Literature and the Values Calculated with the Three Studied EoSs at T = 293.15 K and T = 313.15 K

		CSD EoS [eq 2]		PR EoS		Stryjek EoS [eq 6]	
reference	no. points	AARD (p)/%	AAD (y_1)	AARD (p)/%	AAD (y_1)	AARD (p)/%	AAD (y_1)
Hu et al.[19]	26	0.73	0.0045	0.68	0.0037	0.80	0.0037
Hu et al.[20]	6	0.82	0.0035	0.68	0.0022	0.69	0.0028
Kou et al.[22]	18	0.89	0.0077	1.03	0.0076	0.88	0.0072

Table 8. B_{blend} [Eq 15] and for C_{blend} [Eq 16] Coefficients for the R32 + R1234ze(E) Binary Mixture

B_1	B_2	B_3	B_4	B_5
−6.2182	−2363.9968	−0.2214	0.4647	42.7494
C_1	C_2	C_3	C_4	C_5
14.7236	5116.0490	0.3192	−0.4754	−100.7246

where R = 8.3145 J·mol^{-1}·K^{-1} is the universal gas constant, v_m is the molar volume, and a and b are the CSD parameters. The CSD parameters a and b for pure fluids show the following temperature dependence

$$a = a_0 \exp[a_1 T/\mathrm{K} + a_2 (T/\mathrm{K})^2] \quad (4)$$

$$b = b_0 + b_1 T + b_2 T^2 \quad (5)$$

Table 5 lists the values for a_i and b_i for R32 and R1234ze(E) adopted in this study.

Moreover, the aforementioned method was used with the Peng−Robinson (PR) EoS[30] and a two-parameter cubic EoS proposed by Stryjek.[31,32] The prediction capability of the cubic EoS proposed by Stryjek was studied for the VLE of mixtures containing low GWP refrigerants, as reported elsewhere.[33,34] The cubic EoS proposed by Stryjek has the following form

$$p = \frac{RT}{(v_m - b)} - \frac{a(T)}{(v_m^2 + b v_m - b^2)} \quad (6)$$

where $a(T)$ is the temperature-dependent parameter and b is a constant parameter. a and b in eq 6 are

$$a(T) = 0.4638 \frac{R^2 T_c^2}{p_c} \alpha(T_r, \omega) \quad (7)$$

$$b = 0.1074 \frac{RT_c}{p_c} \quad (8)$$

where T_c is the critical temperature, p_c is the critical pressure, and $\alpha(T_r, \omega)$ is a dimensionless function of the reduced temperature ($T_r = T \cdot T_c^{-1}$) and acentric factor (ω). The α function used in this work is equal to

$$\alpha(T_r, \omega) = [1 + k(1 - T_r)^{0.5}]^2 \quad (9)$$

where k is expressed as

$$k = 0.3577 + 1.4713 \cdot \omega - 0.1665 \cdot \omega^2 + 0.0183 \cdot \omega^3 \quad (10)$$

The three EoSs were extended to the studied mixtures through van der Waals one-fluid mixing rules[35] with a single binary interaction parameter (k_{12}).

As explained elsewhere,[29,36] the "flash method" provides the calculated p and the calculated mole fractions of the liquid phase ($x_{i,calc}$) and the vapor phase ($y_{i,calc}$) for each isochoric measurements by guaranteeing the isofugacity conditions and the minimization of the difference between the calculated volume and experimental volume (V_{iso}), estimated by gravimetric calibration. In particular, the calculation is performed by fixing T, z_i, and n equal to the experimental values. Instead, the values of k_{12} were calculated from the minimization of the following objective function

$$Q = \sum_{i=1}^{N} \left(\frac{p_{exp,i} - p_{calc,i}}{p_{exp,i}} \right)^2 \quad (11)$$

where N is the number of experimental data. This method needs the volumetric properties of liquid and vapor phases for the volume condition, and they were calculated from the EoSs.

Because they provided higher pressure deviations, some two-phase points in the proximity of the change of phase (denoted in Table 3 with a "b") were not considered in the "flash method" calculations.

The average k_{12} for the "flash method" with the CSD EoS was found to be equal to 0.0004, providing an average absolute relative deviation of the pressure (AARD (p)) equal to 0.63%. The AARD (p) was calculated with the following equation

$$\mathrm{AARD}(p)/\% = \frac{100}{N} \sum_{i=1}^{N} \left| \frac{p_{exp,i} - p_{calc,i}}{p_{exp,i}} \right| \quad (12)$$

The average values of k_{12} for the "flash method" with the PR and the cubic EoS proposed by Styjek[31,32] were found to be equal to 0.02047 and 0.01838, respectively, yielding an AARD (p) = 0.46% for the former EoS and AARD (p) = 0.45% for the latter EoS.

The pressures and compositions of liquid and vapor phases derived from the "flash method" with the three EoSs are reported in Table 6. Instead, Figure 3 shows the relative deviations between the measured pressures and the values provided by the selected EoSs. From Figure 3, it is possible to state that the selected EoSs gave comparable and accurate predictions because only few data of the series showed pressure deviations higher than 1%. In particular, it is noted that the cubic EoS proposed by Stryjek and the PR EoS provided slightly lower pressure deviations for the studied systems.

In addition, a comparison between the measured pressures and the pressure predictions of REFPROP 10.0[23] was carried out, providing an AARD (p) equal to 2.16%. The REFPROP 10.0[23] predictions are calculated from EoSs explicit in the reduced Helmholtz energy.[37] The relative deviations between the experimental pressures and the values calculated with REFPROP 10.0 are shown in Figure 3. From Figure 3, it is possible to state that the pressures predicted by REFPROP 10.0 are always higher than the experimental values and less accurate than those calculated with the EoSs, especially at low temperatures where the pressure deviations exceeded 3% for some series.

The VLE behaviors of the R32 + R1234ze(E) binary mixture estimated with the CSD Eos (k_{12} = 0.0004), PR EoS (k_{12} =

https://dx.doi.org/10.1021/acs.jced.9b00995
J. Chem. Eng. Data 2020, 65, 1554−1564

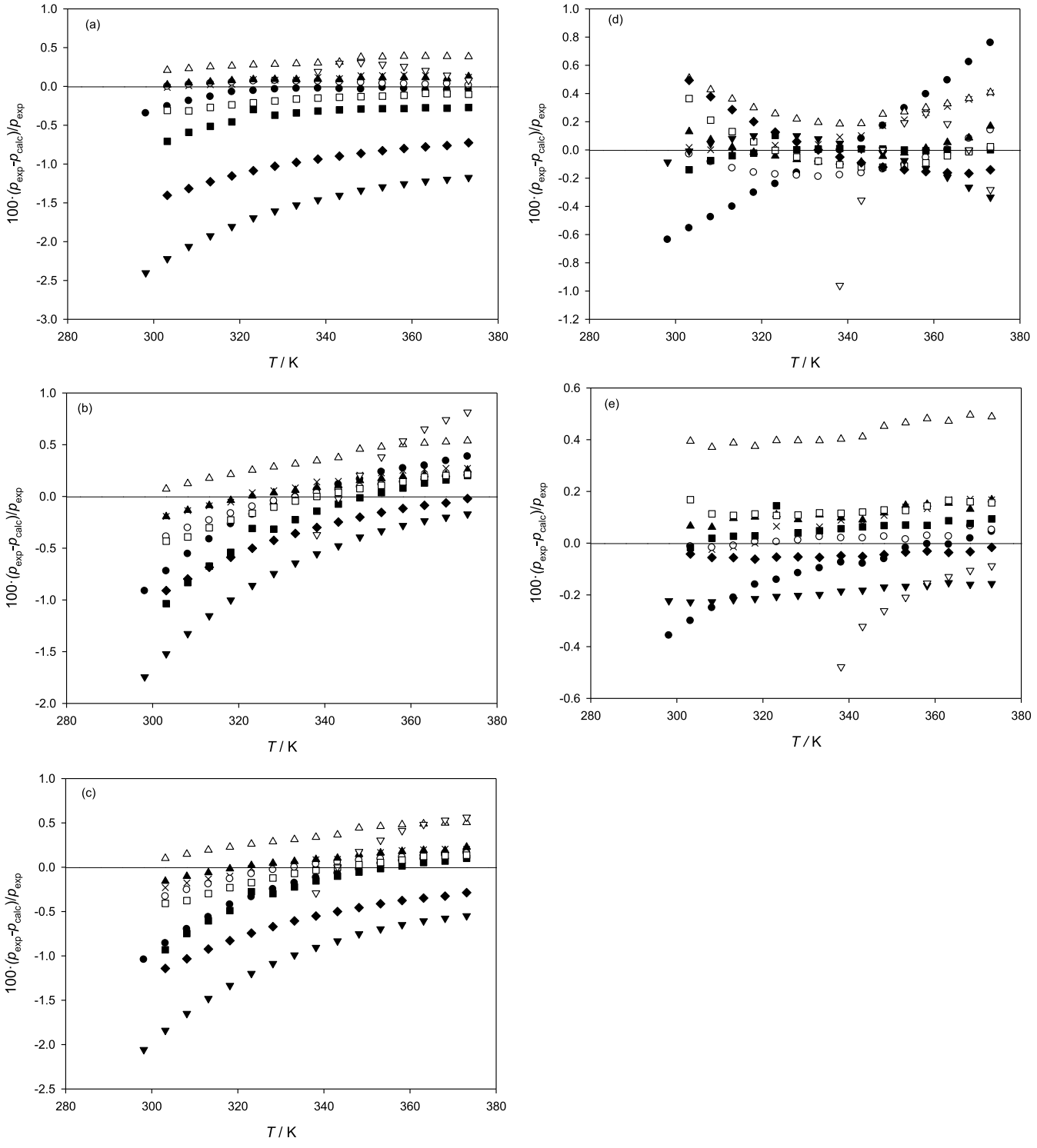

Figure 5. Deviations between the measured pressures for the R32 (1) + R1234ze(E) (2) binary system given in Table 4 (p_{exp}) and the values calculated (p_{calc}) from the CSD EoS (a), the PR EoS (b), a cubic EoS proposed by Stryjek (c), the truncated virial EoS (d), and REFPROP 10.0 (e). ●, z_1 = 0.1677 and v = 0.046522 $m^3 \cdot kg^{-1}$; ×, z_1 = 0.2360 and v = 0.121732 $m^3 \cdot kg^{-1}$; ▽, z_1 = 0.2551 and v = 0.013173 $m^3 \cdot kg^{-1}$; O, z_1 = 0.4634 and v = 0.068959 $m^3 \cdot kg^{-1}$; ▲, z_1 = 0.5374 and v = 0.110447 $m^3 \cdot kg^{-1}$; △, z_1 = 0.6715 and v = 0.115156 $m^3 \cdot kg^{-1}$; ■, z_1 = 0.7383 and v = 0.039422 $m^3 \cdot kg^{-1}$; □, z_1 = 0.7544 and v = 0.068225 $m^3 \cdot kg^{-1}$; ▼, z_1 = 0.9532 and v = 0.043115 $m^3 \cdot kg^{-1}$; ◆, z_1 = 0.9533 and v = 0.062966 $m^3 \cdot kg^{-1}$.

0.02047), and cubic EoSs proposed by Stryjek (k_{12} = 0.01838) at 293.15 and 313.15 K are shown in Figure 4. Moreover, the experimental VLE data for the studied binary mixture available in the open literatures[19,20,22] at the studied temperatures are shown in Figure 4. From this figure, a high level of agreement between the VLE obtained from the studied EoSs and the experimental data is evident. Moreover, the agreement between the calculated and experimental VLE data at the studied temperature is also confirmed by the AARD (p) and the average absolute deviations of the vapor mole fractions (AAD (y_1)) reported in Table 7. In particular, the AAD (y_1) is defined as

https://dx.doi.org/10.1021/acs.jced.9b00995
J. Chem. Eng. Data 2020, 65, 1554−1564

$$\mathrm{AAD}\ (y_1) = \frac{\sum_{i=1}^{N} |y_{1,\mathrm{exp},i} - y_{1,\mathrm{calc},i}|}{N} \quad (13)$$

***pvTz* Calculation.** The measured vapor phase *pvTz* of the R32 + R1234ze(E) binary system was correlated with CSD EoS,[28] PR EoS,[30] the cubic EoS proposed by Stryjek,[31,32] and a virial EoS truncated at the second order. In addition, the experimental data were compared with the REFPROP 10.0[23] predictions. Because they gave higher pressure deviations, the vapor-phase points in the proximity of the change of phase (denoted in Table 4 with a "b") were neglected in the data elaboration.

The van der Waals one-fluid mixing rules[35] were used to extend the CSD EoS,[28] the PR EoS,[30] and the cubic EoS proposed by Stryjek[31,32] to the studied binary mixture. The values of k_{12} obtained from the minimization of AARD (p) were found to be −0.08258 for the CSD Eos, 0.06522 for the PR EoS, and −0.02101 for the cubic EoS proposed by Stryjek, yielding AARD (p) = 0.41% for the CSD EoS, AARD (p) = 0.31% for the PR EoS, and AARD (p) = 0.35% for the Stryjek EoS.

The virial EoS truncated at the second order used to correlate the measurements of Table 4 has the following form

$$p = \frac{RT}{v_m}\left(1 + \frac{B_{\mathrm{blend}}}{v_m} + \frac{C_{\mathrm{blend}}}{v_m^{\,2}}\right) \quad (14)$$

where B_{blend} is the second virial coefficient and C_{blend} is the third virial coefficient. As described in previous papers,[26,27,38] the equations of B_{blend} and C_{blend} are defined as follow

$$B_{\mathrm{blend}} = B_1 \ln(T/K) + \frac{B_2}{T} + B_3 x_1^{\,2} + B_4 x_1 + B_5 \quad (15)$$

$$C_{\mathrm{blend}} = C_1 \ln(T/K) + \frac{C_2}{T} + C_3 x_1^{\,2} + C_4 x_1 + C_5 \quad (16)$$

Table 8 reports the B and C coefficients obtained by minimizing the AARD (p) for the selected vapor-phase data. The AARD (p) between the experimental data of the R32 + R1234ze(E) binary system and the values provided by the truncated virial EoS is 0.16%.

Then, the experimental vapor-phase pressures were compared with the values given by REFPROP 10.0,[23] providing an AARD (p) = 0.14%.

Figure 5 shows the relative deviations between the experimental and the calculated pressures. From Figure 5, it is possible to state that an accurate vapor-phase *pvTz* description of the studied mixtures was given by all the selected models. In particular, the truncated virial EoS and REFPROP 10.0 provided the best results, ensuring deviations within ±1% for all the series. Instead, the other EoSs gave higher deviations, especially for the points at low temperatures, but their results were still accurate.

Because the *pvTz* measurements presented by Kobayashi et al.[18] are not accessible, they were not compared with our experimental data.

CONCLUSIONS

In this paper, 182 two-phase and vapor-phase *pvTz* measurements for the R32 + R1234ze(E) binary system are reported. The flash method with three EoSs was used to derive the VLE behavior of this binary mixture from the experimental points in the two-phase region. This method with the CSD EoS, the PR EoS, and a cubic EoS presented by Stryjek gave AARD (p) of 0.63, 0.46, and of 0.45%, respectively, proving the accuracy of the EoSs in the VLE assessment. Moreover, the calculated VLE agreed with the experimental VLE data collected from the open literature. The vapor-phase *pvTz* data were compared with the values provided by different models. It was found that the AARD (p) equals 0.41% for the CSD EoS, 0.31% for PR EoS, 0.35% for Stryjek EoS, 0.16% for virial EoS, and 0.14% for REFPROP 10.0. The results showed the accuracy of the *pvTz* properties measured in the superheated vapor region.

AUTHOR INFORMATION

Corresponding Author

Giovanni Di Nicola − *Dipartimento di Ingegneria Industriale e Scienze Matematiche, Università Politecnica delle Marche, 60131 Ancona, Italy*; orcid.org/0000-0001-9582-8764; Phone: +39 071 2204277; Email: g.dinicola@univpm.it; Fax: +39 071 2204770

Authors

Sebastiano Tomassetti − *Dipartimento di Ingegneria Industriale e Scienze Matematiche, Università Politecnica delle Marche, 60131 Ancona, Italy*

Uthpala A. Perera − *Kyushu University Program for Leading Graduate School, Green Asia Education Center Interdisciplinary Graduate School of Engineering Sciences and Interdisciplinary Graduate School of Engineering Sciences, Kyushu University, 812-8581 Fukuoka, Japan*

Mariano Pierantozzi − *Dipartimento di Ingegneria Industriale e Scienze Matematiche, Università Politecnica delle Marche, 60131 Ancona, Italy*

Yukihiro Higashi − *International Institute for Carbon-Neutral Energy Research (WPI-I2CNER), Kyushu University, 812-8581 Fukuoka, Japan*

Kyaw Thu − *International Institute for Carbon-Neutral Energy Research (WPI-I2CNER) and Interdisciplinary Graduate School of Engineering Sciences, Kyushu University, 812-8581 Fukuoka, Japan*

Complete contact information is available at: https://pubs.acs.org/10.1021/acs.jced.9b00995

Notes

The authors declare no competing financial interest.

ACKNOWLEDGMENTS

This work was supported by the MIUR of Italy within the framework of the PRIN2015 project "Clean Heating and Cooling Technologies for an Energy Efficient Smart Grid", Prot. 2015M852PA. C.U.A. Perera and K.T. gratefully acknowledge the Kyushu University Program for Leading Graduate School, Green Asia Education Center, for the financial support to conduct this study.

REFERENCES

(1) The Kigali Amendment. *The Amendment to the Montreal Protocol Agreed by the Twenty-Eighth Meeting of the Parties*; UNEP Ozone Secr, 2016.

(2) United Nations. *Paris Agreement*; United Nations Framework Convention on Climate Change, 2015.

(3) Regulation (EU) no. 517/2014 of the European Parliament and of the Council of 16 April 2014 on Fluorinated Greenhouse Gases and Repealing Regulation (EC) no. 842/2006 Text with EEA Relevance.

(4) Ministry of Environment Government of Japan. *Revised F-Gas Law in Japan*, 2015.
(5) The Japan Refrigeration and Air Conditioning Industry Association. Research Projects. 2016.
(6) New Energy and Industrial Technology Development Organization (NEDO). About NEDO. 2016.
(7) McLinden, M. O.; Kazakov, A. F.; Steven Brown, J.; Domanski, P. A. A Thermodynamic Analysis of Refrigerants: Possibilities and Tradeoffs for Low-GWP Refrigerants. *Int. J. Refrig.* **2014**, *38*, 80.
(8) McLinden, M. O.; Brown, J. S.; Brignoli, R.; Kazakov, A. F.; Domanski, P. A. Limited Options for Low-Global-Warming-Potential Refrigerants. *Nat. Commun.* **2017**, *8*, 14476.
(9) Domanski, P. A.; Brignoli, R.; Brown, J. S.; Kazakov, A. F.; McLinden, M. O. Low-GWP Refrigerants for Medium and High-Pressure Applications. *Int. J. Refrig.* **2017**, *84*, 198−209.
(10) Bell, I. H.; Domanski, P. A.; McLinden, M. O.; Linteris, G. T. The Hunt for Nonflammable Refrigerant Blends to Replace R-134a. *Int. J. Refrig.* **2019**, *104*, 484−495.
(11) Brown, J. S. Introduction to Hydrofluoro-Olefin Alternatives for High Global Warming Potential Hydrofluorocarbon Refrigerants Introduction to Hydrofluoro-Olefin Alternatives for High Global Warming Potential Hydrofluorocarbon Refrigerants. *HVACR Res.* **2013**, *19*, 693−704.
(12) Koyama, S.; Takata, N.; Fukuda, S. Drop-in Experiments on Heat Pump Cycle Using HFO-1234ze(E) and Its Mixtures with HFC-32. *International Refrigeration and Air Conditioning Conference*, 2010; pp 1−7.
(13) Tanaka, K.; Higashi, Y. PρTProperty Measurements for Trans -1,3,3,3-Tetrafluoropropene (HFO-1234ze(E)) in the Gaseous Phase. *J. Chem. Eng. Data* **2010**, *55*, 5164−5168.
(14) Bobbo, S.; Nicola, G. D.; Zilio, C.; Brown, J. S.; Fedele, L. Low GWP Halocarbon Refrigerants: A Review of Thermophysical Properties. *Int. J. Refrig.* **2018**, *90*, 181−201.
(15) Tillner-Roth, R.; Yokozeki, A. An International Standard Equation of State for Difluoromethane (R-32) for Temperatures from the Triple Point at 136.34 K to 435 K and Pressures up to 70 MPa. *J. Phys. Chem. Ref. Data* **1997**, *26*, 1273−1328.
(16) Jia, T.; Bi, S.; Hu, X.; Meng, X.; Wu, J. Volumetric Properties of Binary Mixtures of {difluoromethane (R32) + Trans-1,3,3,3-Tetrafluoropropene (R1234ze(E))} at Temperatures from 283.15 K to 363.15 K and Pressures up to 100 MPa. *J. Chem. Thermodyn.* **2016**, *101*, 54.
(17) Tanaka, K.; Akasaka, R.; Higashi, Y. Measurements of Density and Isobaric Specific Heat Capacity for HFO-1234ze (E)+ HFC-32 Mixtures. *Trans. JSRAE* **2011**, *28*, 427−434.
(18) Kobayashi, K.; Tanaka, K.; Higashi, Y. Measurement of PρTx Properties of HFO-1234ze (E) + HFC-32 Mixed Refrigerant. In *Proceedings of the Japan Society of Refrigerating and Air Conditioning Engineers*; Japan Society of Refrigerating and Air Conditioning Engineers, 2011; Vol. *28*, pp 415−426.
(19) Hu, X.; Meng, X.; Wu, J. Isothermal Vapor Liquid Equilibrium Measurements for Difluoromethane (R32) + Trans-1,3,3,3-Tetrafluoropropene (R1234ze(E)). *Fluid Phase Equilib.* **2017**, *431*, 58−65.
(20) Hu, X.; Yang, T.; Meng, X.; Bi, S.; Wu, J. Vapor Liquid Equilibrium Measurements for Difluoromethane (R32) + 2,3,3,3-Tetrafluoroprop-1-Ene (R1234yf) and Fluoroethane (R161) + 2,3,3,3-Tetrafluoroprop-1-Ene (R1234yf). *Fluid Phase Equilib.* **2017**, *438*, 10−17.
(21) Koyama, S.; Matsuo, Y.; Fukuda, S.; Akasaka, R. Measurement of Vapor-Liquid Equilibrium of HFO-1234ze (E)/HFC-32. In *Proceedings 2010 JSRAE Annual Conference*: Kanazawa, Japan; 2010; p B111.
(22) Kou, L.; Yang, Z.; Tang, X.; Zhang, W.; Lu, J. Experimental Measurements and Correlation of Isothermal Vapor-Liquid Equilibria for HFC-32+ HFO-1234ze (E) and HFC-134a+ HFO-1234ze (E) Binary Systems. *J. Chem. Thermodyn.* **2019**, *139*, 105798.
(23) Lemmon, E. W.; Bell, I. H.; Huber, M. L.; McLinden, M. O. *NIST Standard Reference Database 23: Reference Fluid Thermodynamic and Transport Properties-REFPROP*, version 10.0; National Institute of Standards and Technology, 2018.
(24) Giuliani, G.; Kumar, S.; Polonara, F. A Constant Volume Apparatus for Vapour Pressure and Gas Phase P-ν-T Measurements: Validation with Data for R22 and R134a. *Fluid Phase Equilib.* **1995**, *109*, 265−279.
(25) Di Nicola, G.; Polonara, F.; Ricci, R.; Stryjek, R. PVTx Measurements for the R116+ CO2 and R41+ CO2 Systems. New Isochoric Apparatus. *J. Chem. Eng. Data* **2005**, *50*, 312−318.
(26) Brown, J. S.; Coccia, G.; Tomassetti, S.; Pierantozzi, M.; Di Nicola, G. Vapor Phase PνTx Measurements of Binary Blends of 2,3,3,3-Tetrafluoroprop-1-Ene + Isobutane and Trans-1,3,3,3-Tetrafluoroprop-1-Ene + Isobutane. *J. Chem. Eng. Data* **2017**, *62*, 3577−3584.
(27) Brown, J. S.; Coccia, G.; Tomassetti, S.; Pierantozzi, M.; Di Nicola, G. Vapor Phase PvTx Measurements of Binary Blends of Trans-1-Chloro-3,3,3-Trifluoroprop-1-Ene + Isobutane and Cis-1,3,3,3-Tetrafluoroprop-1-Ene + Isobutane. *J. Chem. Eng. Data* **2018**, *63*, 169−177.
(28) De Santis, R.; Gironi, F.; Marrelli, L. Vapor-Liquid Equilibrium from a Hard-Sphere Equation of State. *Ind. Eng. Chem. Fundam.* **1976**, *15*, 183−189.
(29) Di Nicola, G.; Giuliani, G.; Passerini, G.; Polonara, F.; Stryjek, R. Vapor-Liquid-Equilibrium (VLE) Properties of R-32 + R-134a System Derived from Isochoric Measurements. *Fluid Phase Equilib.* **1998**, *153*, 143−165.
(30) Peng, D.-Y.; Robinson, D. B. A New Two-Constant Equation of State. *Ind. Eng. Chem. Fundam.* **1976**, *15*, 59−64.
(31) Stryjek, R. Correlation and Critical-Evaluation of Vle Data for Nitrogen+ Argon, Nitrogen+ Methane, and Argon+ Methane Mixtures. *Bull. Pol. Acad. Sci.* **1991**, *39*, 353−361.
(32) Stryjek, R. On the prediction of the gas-liquid critical locus with cubic equations of state. *Bull. Pol. Acad. Sci.* **1992**, *40*, 211−220.
(33) Nicola, G. D.; Coccia, G.; Pierantozzi, M.; Tomassetti, S. Vapor-Liquid Equilibrium of Binary Systems Containing Low GWP Refrigerants with Cubic Equations of State. *Energy Procedia* **2018**, *148*, 1246−1253.
(34) Di Nicola, G.; Coccia, G.; Pierantozzi, M.; Tomassetti, S.; Stryjek, R. Analysis of Vapor Pressure and VLE of HFOS, HCFOS, and Their Blends with Cubic Equations of State. In *Refrigeration Science and Technology*; International Institute of Refrigeration, 2018; Vol. Part F1476, pp 403−412.
(35) Poling, B. E.; Prausnitz, J. M.; O'Connell, J. P. *The Properties of Gases and Liquids*, 5th ed.; McGraw-Hill, 2004.
(36) Tomassetti, S.; Coccia, G.; Pierantozzi, M.; Di Nicola, G.; Brown, J. S. Vapor Phase and Two-Phase PvTz Measurements of Difluoromethane+ 2, 3, 3, 3-Tetrafluoroprop-1-Ene. *J. Chem. Thermodyn.* **2020**, *141*, 105966.
(37) Bell, I. H.; Lemmon, E. W. Automatic Fitting of Binary Interaction Parameters for Multi-Fluid Helmholtz-Energy-Explicit Mixture Models. *J. Chem. Eng. Data* **2016**, *61*, 3752−3760.
(38) Tomassetti, S.; Pierantozzi, M.; Di Nicola, G.; Polonara, F.; Brown, J. S. Vapor-Phase PvTx Measurements of Binary Blends of Cis-1, 2, 3, 3, 3-Pentafluoroprop-1-Ene+ Isobutane and 3, 3, 3-Trifluoropropene+ Isobutane. *J. Chem. Eng. Data* **2019**, *64*, 688.

https://dx.doi.org/10.1021/acs.jced.9b00995
J. Chem. Eng. Data 2020, 65, 1554−1564